Newcastle University

ePrints

Al-Abduly A, Christensen P, Harvey A, Zahng K. Characterization and optimization of an oscillatory baffled reactor (OBR) for ozone-water mass transfer. *Chemical Engineering and Processing: Process Intensification* 2014, 84, 82-89.

Copyright:

© 2014. This manuscript version is made available under the CC-BY-NC-ND 4.0 license

DOI link to article:

http://dx.doi.org/10.1016/j.cep.2014.03.015

Date deposited:

09/02/2016

Embargo release date:

08 April 2015

This work is licensed under a
Creative Commons Attribution-NonCommercial-NoDerivatives 4.0 International licence

Newcastle University ePrints - eprint.ncl.ac.uk

This work was requested for the special issue EPIC 2013 to be edited by Tom van Gerven.

Characterization and optimization of an oscillatory baffled reactor (OBR) for ozone - water mass transfer

Abdullah Al-Abduly*

School of Chemical Engineering and Advanced Materials, Bedson Building, Newcastle University, Newcastle upon Tyne, NE1 7RU, United Kingdom
Phone: + 44 (0) 1912087056, Mobile phone: +44 (0) 7588339292
Email: a.j.h.al-abduly@ncl.ac.uk

Paul Christensen

School of Chemical Engineering and Advanced Materials, Bedson Building, Newcastle University, Newcastle upon Tyne, NE1 7RU, United Kingdom
Phone: + Phone: +44 (0) 191 208 5472
Email: paul.christensen@newcastle.ac.uk

Adam Harvey

School of Chemical Engineering and Advanced Materials, Newcastle University, Newcastle upon Tyne, NE1 7RU, United Kingdom
Phone: +44 (0) 191 208 7268
Email: adam.harvey@newcastle.ac.uk

Kui Zahng

School of Chemical Engineering and Advanced Materials, Newcastle University, Newcastle upon Tyne, NE1 7RU, United Kingdom
Email: kui.zhang@newcastle.ac.uk

Abstract

Ozone-water mass transfer was investigated using an oscillatory baffled reactor (OBR) operated as a semi-batch and as a co-current up flow continuous reactor. The effects of input ozone concentration, input gas and water flow rates, and oscillation conditions on gas hold up, volumetric mass transfer coefficient and mass transfer efficiency were determined. The same reactor was operated as a baffled column (without oscillation) and as a bubble column to assess the effect of the reactor arrangement on the mass transfer. The results show that the OBR was 5 and 3 times more efficient for ozone-water mass transfer than the baffled and bubble column reactors, respectively. The enhancement obtained with OBR over the baffled column reactor for ozone-water mass transfer was found to decrease with gas flow rate due to changes in bubble flow pattern from homogenous to heterogeneous. Under continuous flow conditions, the performance of the baffled reactor and the OBR were found to be twice efficient for ozone-water mass transfer than when operating under semi-batch conditions. The mass transfer effeciency (*MTE)* was found to increase from 57 % using the baffled reactor to 92 % with OBR under continuous flow at water and gas superficial velocities of 0.3 and 3.4 cm s^{-1}, respectively.

Keywords: ozone dissolution, mass transfer, oscillatory baffled reactor, continuous flow.

1. Introduction

Ozone is generally believed to be a strong oxidant and is employed in water and waste water treatment due to its high oxidation potential and ability to remove a wide range of chemical and biological contaminants [1-4]. However, the main shortcoming of ozone is its low solubility in water which limits the extent of its application. Hence, several techniques have been employed for improving ozone-water mass transfer including bubble columns, stirred tanks, and packed columns [5-10]. Oscillatory Baffled Reactors (OBR's) have shown promising performance toward the dissolution of oxygen in water [11-13]. OBRs were found to enhance the dissolution of oxygen in water 6 times faster than bubble columns [12], and to be 75% more power efficient than stirred vessels [13]. Unlike most gas-liquid contactors the diffuser type had no effect on OBR efficiency [11], and this may be considered as a unique feature of this type of reactors.

Oscillatory baffled reactors consist of a column within which are mounted a series of baffles dividing the column into cells. The oscillation of the liquid within the OBR is generated by a piston or bellows mounted at one end of the OBR. Gas-liquid mixing in OBRs takes place via the formation of vortices or eddies between each pair of baffles, and the size and intensity of these eddies depends on the baffle geometries and oscillation frequency and amplitude [12, 14, 15]. The oscillatory Reynolds number (Re_o) is normally used to describe the mixing condition in OBRs, while the Strouhal number (St) measures the efficiency of eddy propagation [12]. These parameters are important characteristics of OBRs, and are calculated using equations (1) and (2), respectively [12, 15, 16]:

$$R_{eo} = \frac{2\pi f X_0 \ pD}{\mu} \qquad (1)$$

$$St = \frac{D}{4\pi x_0} \quad (2)$$

where f is the oscillation frequency (Hz), x_o the oscillation amplitude centre to peak (m), p is the liquid density (kg m^{-3}), μ is the liquid viscosity (kg m s^{-1}) and D is the column inner diameter (m).

The aim of this work was to examine the performance of an oscillatory baffled reactor for ozone-water mass transfer under semi-batch and continuous flow conditions to understand the effects of operational conditions on the mass transfer. The main objectives were to determine the effects of the reactor arrangement, input ozone concentration, input gas and water flow rates and oscillation conditions on gas hold up, bubble size, volumetric mass transfer coefficient (k_La) and mass transfer efficiency (*MTE*).

2. Experimental

2.1 The experimental setup

The system shown in fig.1 consists of a jacketed column, 190 cm in length and 2.5 cm in internal diameter (*D*), which was mounted vertically on an oscillation-inducing motor. The column contained orifice-type baffles made of 2.0 mm thick stainless steel with an outer diameter of 24 mm and inner diameter (D_o) 12.5 mm. The baffles were fixed along the column using two stainless steel rods of diameter 2.0 mm, and the distance separating each pair of baffles was 37.5 mm. These baffle geometries were chosen in order to maintain optimal mixing [14]. The fluid oscillation motion was provided by a motor connected to a piston fixed at the bottom of the column. The oscillation frequency and amplitude were adjusted using control units connected to the motor. As can be seen in fig.1, the column had two inlets at the bottom for ozone and water, and a sampling port located 90 cm from the column bottom.

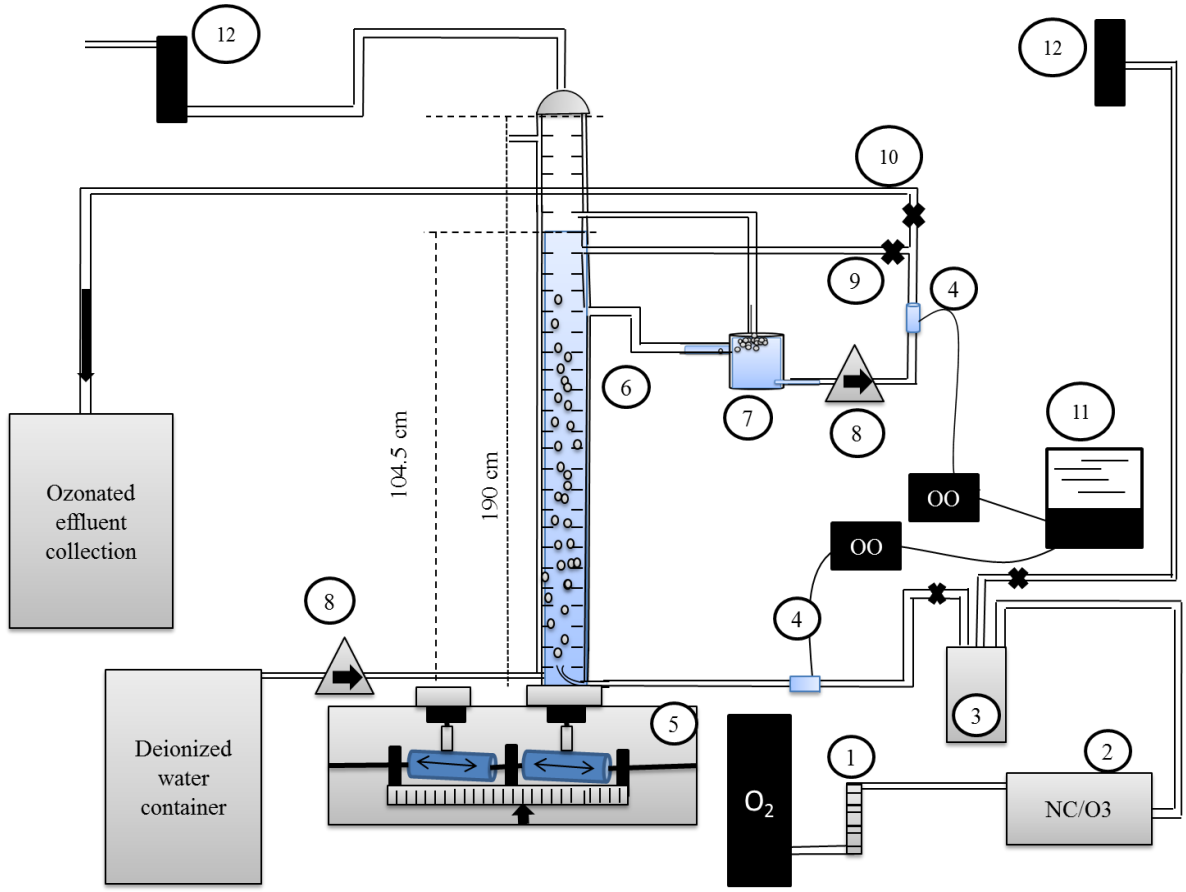

Figure 1 The system setup: (1) gas flow meter, (2) novel cell-ozone generator (PBDBD), (3) ozone distribution cell, (4) Ocean Optics flow cells, (5) oscillation supplying motor, (7) bubble removing cell, (8) peristaltic tubing pumps, (9) return port, (10) outlet port, (11) data collection station and (12) ozone destruction cells.

Ozone was passed through an ozone distribution cell placed prior to the reactor to control the direction of the input gas flow. The distribution cell consists of one inlet channel for the ozone feed and two outputs each with a valve for gas release. As can be seen in fig.1, one of the output channels was connected to the flow cell of an Ocean Optics Spectrometer positioned prior to the OBR while the other one was directed to an ozone catalytic destruction cell. The ozone distribution cell was included to allow the ozone generator to reach the steady state before ozone was introduced into the reactor through the bottom of the OBR.

The instantaneous change in the dissolved ozone concentration was monitored by passing the sampled water at a pre-set flow rate through an Ocean Optics spectrometer flow cell (10 mm

optical pathlength). The water sampling rate was maintained using a calibrated peristaltic pump (520S/R, Watson-Marlow). A bubble-removing cell was placed prior to the flow cell to remove any remaining bubbles from the sample before analysis. The released gas was returned back to the column through a gas returning port located 35 cm above the sampling port. The water was then passed either back to the column through a water return port located 15 cm above the sampling port, or to an external tank, depending on the type of experiment performed. The volume of water occupying the analytical cycle including the bubble-removing cell, was 57 cm^3, and the actual volume within the column at any time during the analysis was 500 cm^3, with a height of 104.5 cm with no aeration at room temperature.

After each run, the feed gas was allowed to pass directly to the ozone destruction cell through the gas distribution cell. The system was purged with oxygen for 10 minutes to remove the dissolved ozone, after which the water was completely removed from the column, and the latter flushed with fresh, deionised water.

All the experimental work described in this paper was performed at room temperature under atmospheric pressure with no pH adjustment, using deionized water from a Millipore Milli-Q system (18.3 MΩ cm). Hence, any complications arising from the presence of ozone-scavenging species were avoided [1, 17].

The range of experimental conditions in terms of the input gas and liquid flow rates, ozone concentrations and oscillation amplitude and frequency in the semi-batch and in continuous flow experiments are shown in tables 1 and 2.

2.2 Ozone generation

Ozone was supplied to the system using a novel, packed beads dielectric barrier discharge generator (PBDBD) developed in-house. The PBDBD consisted of two high voltage electrodes separated by a layer of glass beads. These components were arranged within a

jacketed cell to allow cooling. The cell was then connected to a cooling system to maintain the temperature at desirable levels. Oxygen was used to feed the generator, and the flow rate was adjusted using a needle valve and monitored with a calibrated gas flow meter (NGX, PLATON). The PBDBD could be operated over a range of oxygen flow rates, and the required ozone concentration was set by controlling the input power. The required time for the generator to reach a steady state with respect to ozone concentration was ca. 5.0 minutes.

2.3 Ozone analysis

The concentration of ozone in the gas phase was monitored online by passing the exhaust gas from the PBDBD through a 10 mm optical pathlength flow cell connected to an Ocean Optics spectrometer (USB2000, Ocean Optics), and the absorbance was monitored at 254 nm. The ozone concentration was calculated using a molar extinction coefficient of 3000 $dm^3\ mol^{-1}\ cm^{-1}$ [18]. Prior to the analysis, the cell was purged with pure oxygen to calibrate the spectrometer background. A similar flow cell was employed for monitoring the instantaneous change in dissolved ozone concentration at 258 nm using a molar extinction coefficient of 2900 $dm^3\ mol^{-1}\ cm^{-1}$ [19] after adjusting the spectrometer background with deionized water.

2.4 Ozone destruction in the effluent gas

For safety purposes, the ozone-containing off gas was passed through a Dreschel bottle filled with a MnO_2-based catalyst to convert the ozone to oxygen [20]. The catalyst, (CARULIT 200), was obtained from Cara Corp, UK, and used without further treatment. The efficiency of the cell toward ozone destruction was confirmed by placing Ocean Optics flow cells before and after the destruction unit.

2.5 Ozone-water volumetric mass transfer coefficient determination (k_La)

The rate of ozone dissolution was determined according to [12]:

$$d[O_3]_L/dt = k_La\ ([O_3]^* - [O_3]_L) \quad (3)$$

which can be integrated and rearranged as follows [12]:

$$Ln\ ([O_3]^* - [O_3]_L) = -\ k_L a\ t + constant \quad (4)$$

where $[O_3]^*$ is the steady state, dissolved ozone concentration (mg dm^{-3}), $[O_3]_L$ the dissolved ozone concentration (mg dm^{-3}) at time t (min) and k_La is the volumetric mass transfer coefficient (min^{-1}).

Table 1: Summary of the experimental conditions employed.

Parameter	*Semi-batch*	*Continuous*
Q_G *(dm³ min⁻¹)*	0.1 - 2.0	0.1 - 1.0
U_G *(cm s⁻¹)*	0.3 - 6.8	0.3 - 3.4
Q_L *(dm³ min⁻¹)*	0.0	0.1 - 1.0
U_L *(cm s⁻¹)*	0.0	0.3 – 3.4
$[O_3]_G$ *(mg dm⁻³)*	11.3 - 64.5	11.3 - 64.5
Sampling rate (dm³ min⁻¹)	0.18	$= Q_L$

Table 2: The oscillation conditions employed in this work.

	Semi-batch	*Continuous*
Frequency (Hz)	1.2 - 5.0	5.0
Amplitude (mm)	1.0 - 6.0	6.0
Re_o	178 - 4600	4600
St	1.99 - 0.33	0.33

3. Results and discussion

3.1 Ozone-water mass transfer in semi-batch conditions

The reactor was operated as a bubble column (with no baffles or oscillation), baffled reactor (without oscillation), and as an OBR (with baffles and oscillation) to establish a base for

comparison between theses arrangements on one hand, and to the available data in the literature on the other.

3.1.1 The effect of applied ozone concentration on ozone-water solubility

The effect of varying the input ozone concentration on the dissolved ozone concentration was investigated employing the baffled reactor with no oscillation or water throughput in order to determine the unperturbed dissolved ozone concentration. Figure 2 shows the change in dissolved ozone concentration as a function of time and input gas phase ozone concentration. As can be seen from fig.2, the steady state dissolved ozone concentration increased as the gas phase ozone concentration increased. In all cases, the dissolved ozone concentration increased rapidly during the first minute, reaching steady state after ca. 2.5 minutes.

The steady state dissolved ozone concentration, k_La and the Henry's Law constant were determined from fig. 2, and these are presented in table 3. The Henry's Law constant (H_o, atm dm^3 mol^{-1}) was evaluated according to:

$$P_{O3} = H_o [O_3]^* / 48000 \quad (6)$$

where P_{O3} is the partial pressure of the input ozone (atm) and $[O_3]^*$ is the steady state dissolved ozone concentration (mg dm^{-3}). From table 3 the steady state dissolved ozone concentration was found to increase linearly with the input ozone concentration. However, the H_o and k_La values so obtained were found to be almost constant and independent of the input ozone concentrations. The Henry's Law constant for ozone-water dissolution was 80.1 ± 5 atm dm^3 mol^{-1}, which was in good agreement with the 79.4 atm dm^3 mol^{-1} observed by Kuosa et al. (2004) [21].

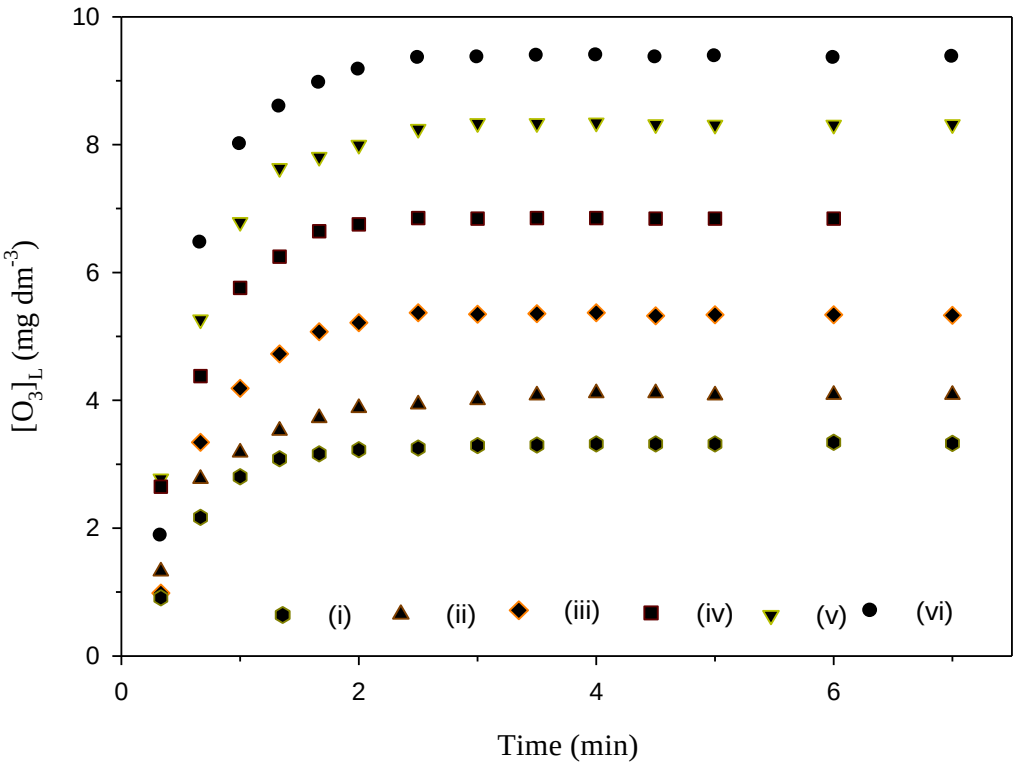

Figure 2 The change in dissolved ozone with time as a function of the input ozone concentration using the baffled reactor. Q_G was 1.0 dm^3 min^{-1} and $[O_3]_G$ were: (i) 11.3, (ii) 13.3, (iii) 18.1, (iv) 22.4, (v) 27.7 and (vi) 33.3 mg dm^{-3}.

Table 3: k_La values at different input ozone concentrations, Q_G = 1.0 dm^3 min^{-1}, using the baffled reactor.

$[O_3]_G$ (mg dm^{-3})	$[O_3]^*$ (mg dm^{-3})	k_La (min^{-1})	Henry's constant (atm dm^3 mol^{-1})
11.3	3.34	1.99	81.4
13.3	4.29	1.99	74.6
18.1	5.37	1.94	81.1
22.4	6.85	1.93	78.7
27.7	8.33	1.91	80.0
33.3	9.39	2.00	85.3

3.1.2 The effect of oscillation on ozone-water mass transfer

In order to evaluate the optimal mixing conditions for ozone mass transfer, the OBR was operated at various oscillation amplitudes and frequencies and the k_La values were recorded.

Figure 3 shows the effect of oscillation on ozone-water mass transfer at a constant input gas flow rate. As can be seen from fig. 3, ozone dissolution was found to increase slightly as Re_o increased from 0 to 1000, however the most important enhancement was observed at Re_o between 3000 and 4600. Because of instrumental limitation, Re could not be increased above 4600. The enhancement observed with increasing the oscillation amplitude and frequency may be attributed to increase bubble break-up [11, 12, 22] induced by increasing the speed and strength of the interaction between the oscillating liquid and the sharp edges of the baffles.

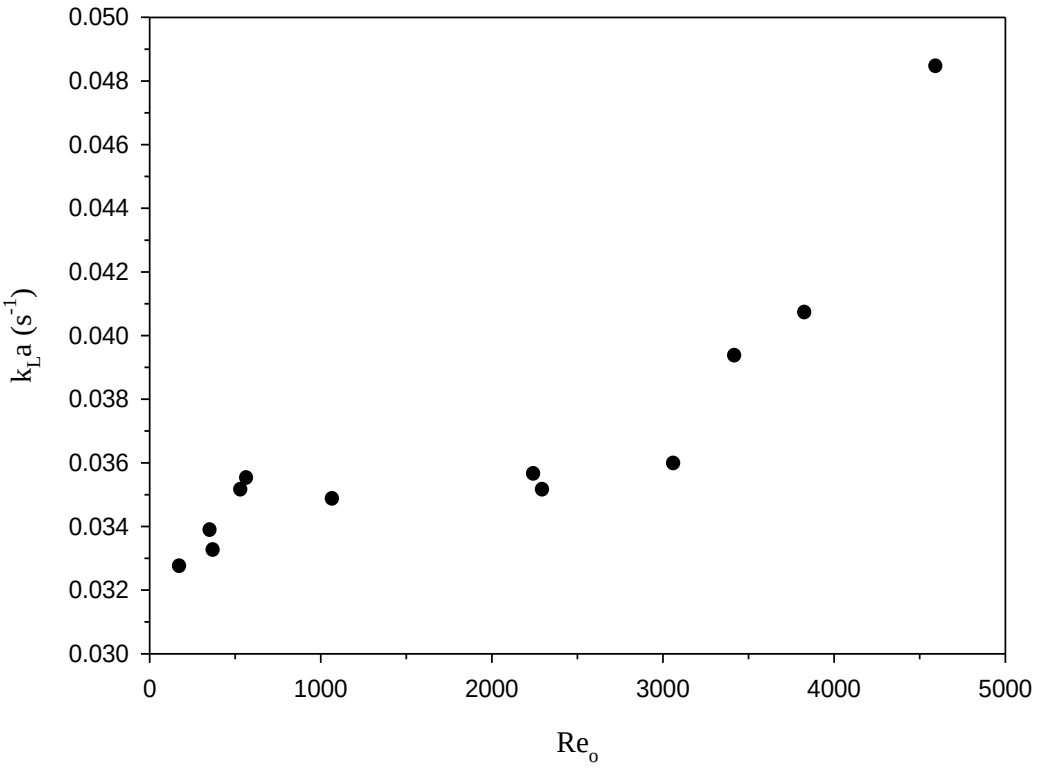

Figure 3 A plot of ozone-water mass transfer coefficient as a function of Re_o. The $[O_3]_G$ was 62.0 mg dm^{-3} and Q_G was 1.0 dm^3 min^{-1}.

3.1.3 The effect of the reactor arrangement on ozone-water mass transfer

The effect of the reactor arrangement on the ozone-water dissolution rate is shown in fig.4. As can be seen, k_La increased in the order: OBR > baffled reactor > bubble column; the value of

k_La observed using the OBR was found to be 5 and 3 times greater, than those observed using the bubble and baffled reactors, respectively. It is interesting to note that, the k_La values observed using the bubble reactor were found to agree with the average results reported previously under similar conditions [7, 8].

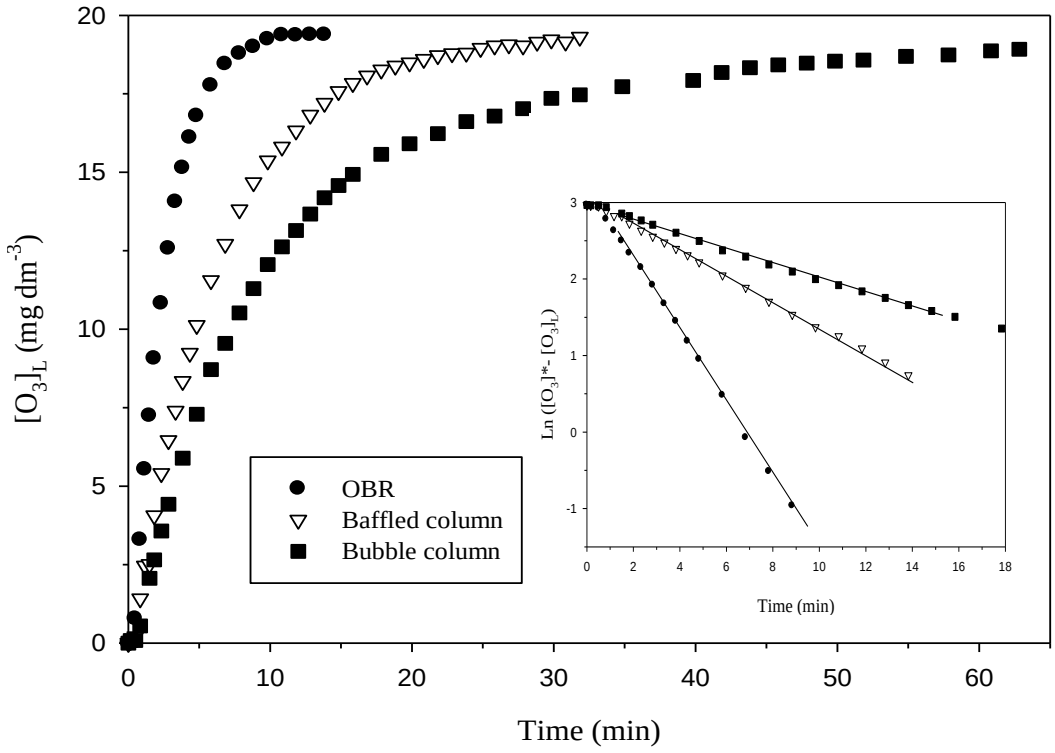

Figure 4 Ozone-water dissolution as a function of running time and reactor arrangement. $[O_3]_G$ was 65 mg dm^{-3} at Q_G = 0.1 dm^3 min^{-1}. Re_o was fixed at 4600 in the case of the OBR. The inset shows the plots of Ln ($[O_3]$-$[O_3]_L$) vs. time used for the determination of k_La (see text for details).*

3.1.4 The effect of the input gas flow rate on ozone-water k_La

The effect of varying the input gas flow rate on the ozone-water mass transfer coefficient obtained using the three reactor arrangements are shown in fig. 5. As can be seen from fig. 5, k_La increased with input gas flow rate regardless of the reactor arrangement. Unexpectedly, the enhancement obtained using the baffled reactor over the bubble column reactor was found to increase from 1.8 to 2.3 times as the input gas superficial velocity increased from 0.34 – 6.8 cm

s^{-1}. In general, the enhancement obtained using the baffled reactor may be attributed to the continuous bubble collisions with the baffles, which reduce the rising velocity of the bubbles and increase their break-up as can be seen in see fig.6 (a). These two factors become more significant as the gas superficial velocity increases, hence increasing the gas hold-up and k_La. This behaviour was not in agreement with that observed by Hewgill and co-workers who found that the baffled reactor was less efficient than bubble column for oxygen-water dissolution [12]. This may be attributed to the lower input gas superficial velocities (i.e 0.042 - 0.24 cm s^{-1}) employed during their investigation compared with those investigated here.

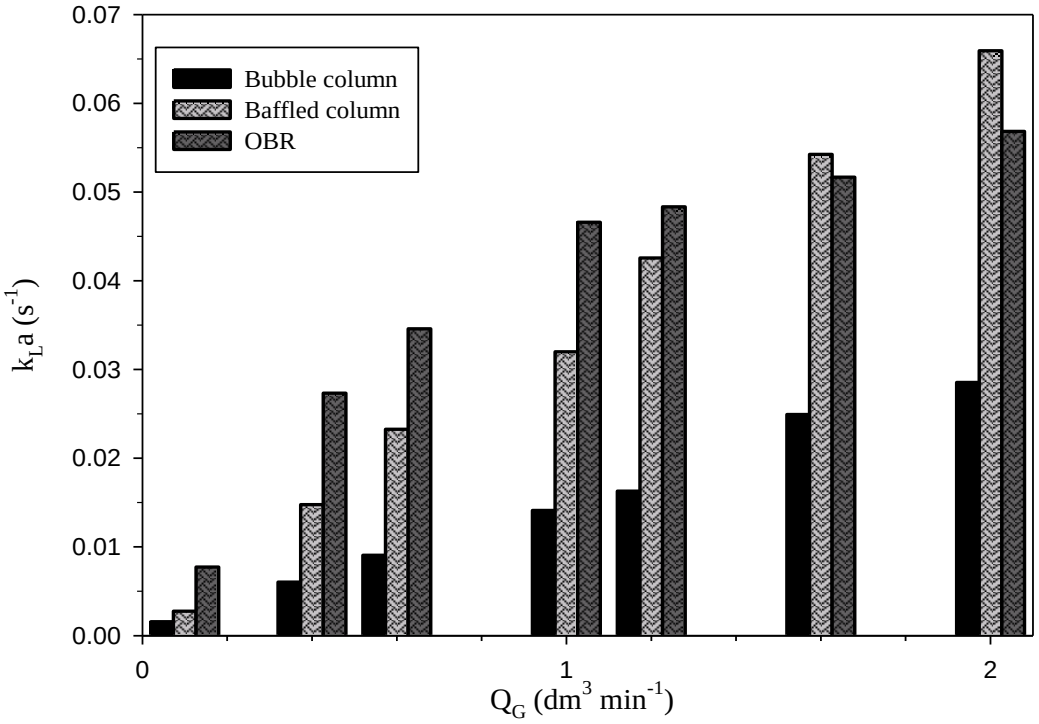

Figure 5 Ozone-water mass transfer coefficients as a function of the reactor arrangement and input gas flow rate. Re_o was fixed at 4600 in the case of the OBR.

From fig. 5, it can be seen that the enhancement in k_La obtained with the OBR at input gas flow rates of 0.1-1.0 dm^3 min^{-1} was more significant than that observed at the higher input gas flow rates of 1.2 - 2.0 dm^3 min^{-1}. However, as the flow rate increased from 1.6 to 2.0 dm^3 min^{-1}, the k_La values observed with the OBR were lower than those obtained using the

baffled reactor. This behaviour may be interpreted by considering the variation of gas flow patterns at high and low flow rates, as shown in figs. 6 (b) and (c).

Figures 6 (a) – (c) show the gas flow patterns observed using the baffled reactor (a) and the OBR operated at low (b) and high (c) input gas flow rates, respectively. Small and homogenously distributed bubbles can be seen in fig. 6 (b), and most of these bubbles were trapped by high speed, circulating vortices, shown by dashed lines in fig. 6 (b) and (c). Larger bubbles were formed within each vortex as a result of bubble collision, and these larger bubbles moved from the centre to the external walls of each vortex. However, the rate of bubble collision was expected to increase with increasing volumetric ratio of gas to liquid, which led to vortex disturbance and reduced the residence time of the bubbles within the reactor as can be seen in fig. 6 (c).

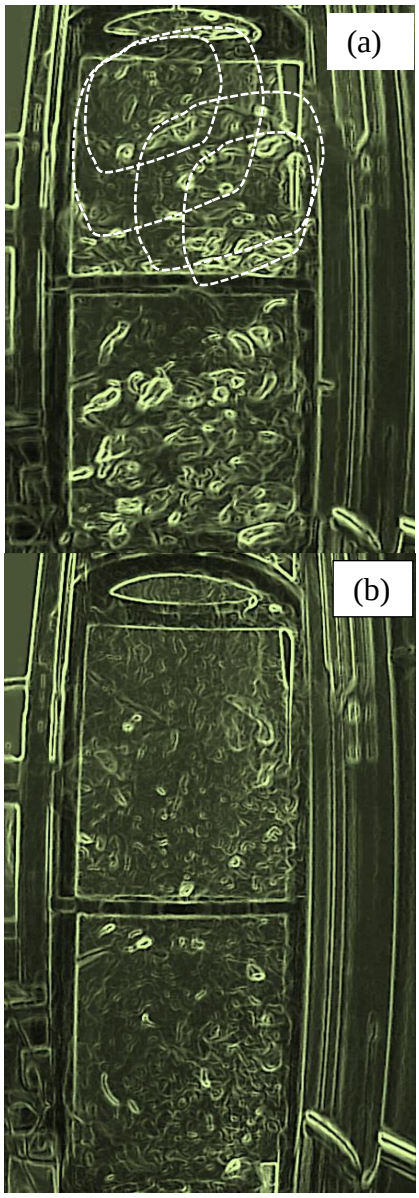

Figure 6 Gas flow patterns observed using the baffled reactor at 0.4 dm^3 min^{-1} (a) and the OBR at 0.4 dm^3 min^{-1}(b) and 1.6 dm^3 min^{-1} (c). The Re_o was fixed at 4600 in both (b) and (c).

3.1.5 Gas hold-up and k_La

The gas hold-up (ε_G), which determines the volumetric fraction of gas within the liquid, is generally well accepted as an important hydrodynamic parameter which describes the effectiveness of gas-liquid contactor toward the mass transfer [22, 23]. Oliveira et al. 2004 [22] have shown that the type of sparger had no effect on mass transfer coefficient in an oscillatory baffled reactor, and this was attributed to the high turbulence caused by liquid oscillation. In the present work, the effect of gas diffuser type on gas hold-up and k_La was

investigated in the absence of oscillation using the baffled reactor. The gas hold up was measured at different input ozone flow rates according to [11]:

$$\varepsilon_G = (h-h_o)/h \quad (8)$$

where h and h_o were the liquid heights (cm) during and before aeration, respectively. Two spargers were employed for this experiment: a perforated PTFE diffuser (A) 12 mm high and 10 mm in diameter with a 1.0 mm pore diameter which produced large bubbles ca. 8.0 mm in diameter, and a stone diffuser (B) with a small pore size producing small bubbles of diameter 0.3-0.1 mm. Figure 7 shows the effect of gas superficial velocity on gas hold-up observed using the two diffusers. As can be seen in fig. 7, a slight and almost constant enhancement of gas hold-up was observed using the diffuser (A) over (B). However, diffuser type has no apparent effect on the volumetric mass transfer coefficient, as depicted in fig. 8. Therefore, the independence of the gas-liquid mass transfer coefficient of OBRs on the diffuser type observed previously [22] can be extended to include baffled reactors.

Figure 9 shows the plot of volumetric mass transfer coefficient as a function of gas hold-up obtained under different operational conditions of reactor arrangement, oscillation condition, sparger type and input gas flow rates. As may be seen from the figure, there is a linear relationship between gas hold-up and mass transfer coefficient. Considering the varity of the operational conditions and bubble size, it does not seem unreasonable to postulate that gas hold-up is the most important factor that controls the ozone-water mass transfer coefficient. This is in agreement with Olivira et al 2004 [11] who have shown that the contribution of gas hold-up on mass transfer coefficient is more significant than bubble size.

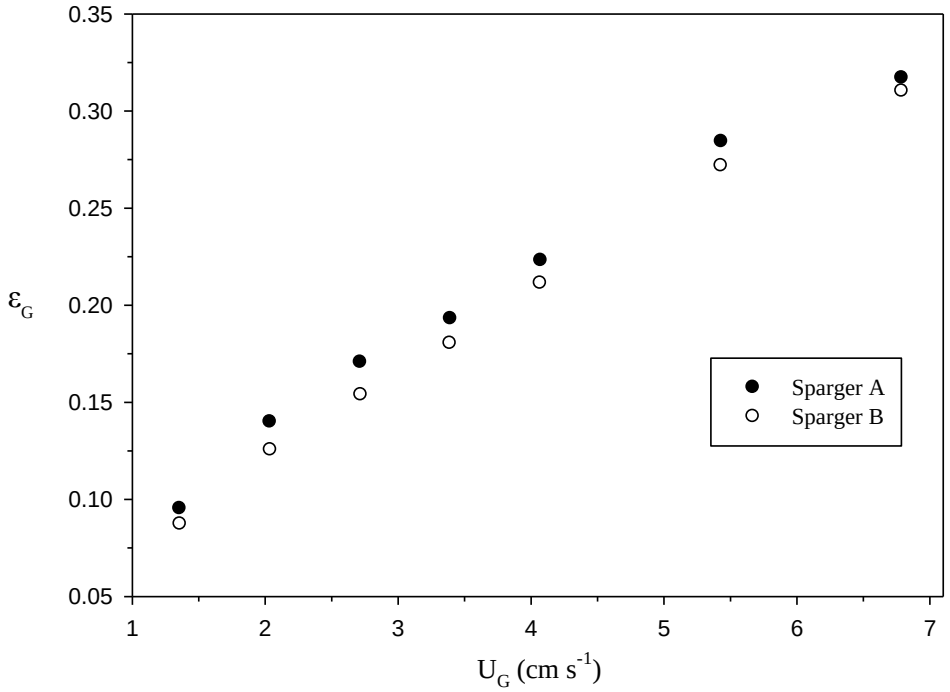

Figure 7 Plot of gas hold-up as a function of the gas superficial velocity obtained using spargers A and B in the baffled reactor.

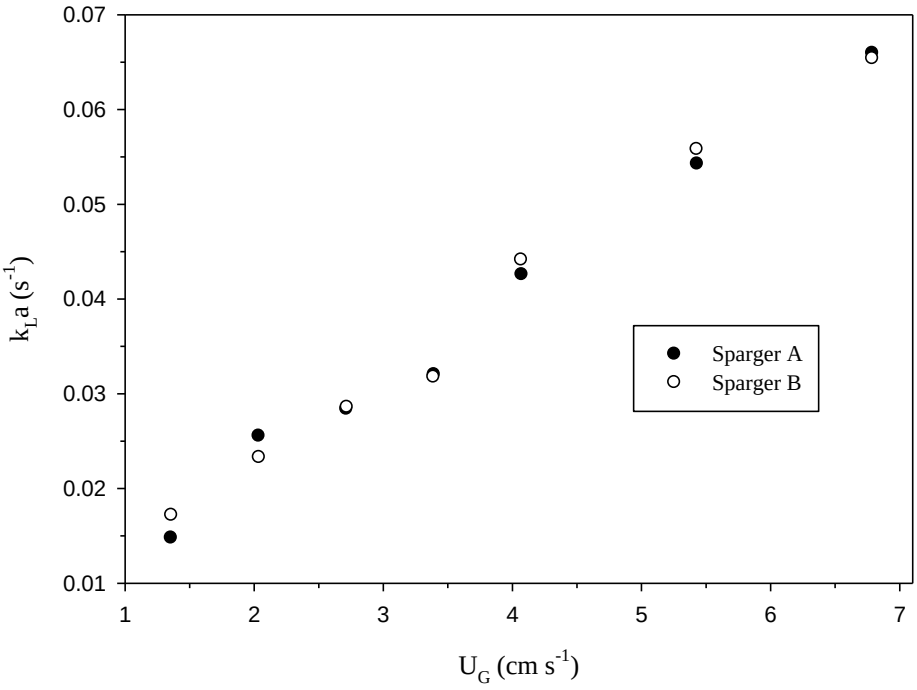

Figure 8 Plot of k_La as a function of gas superficial velocity and diffuser type using the baffled reactor.

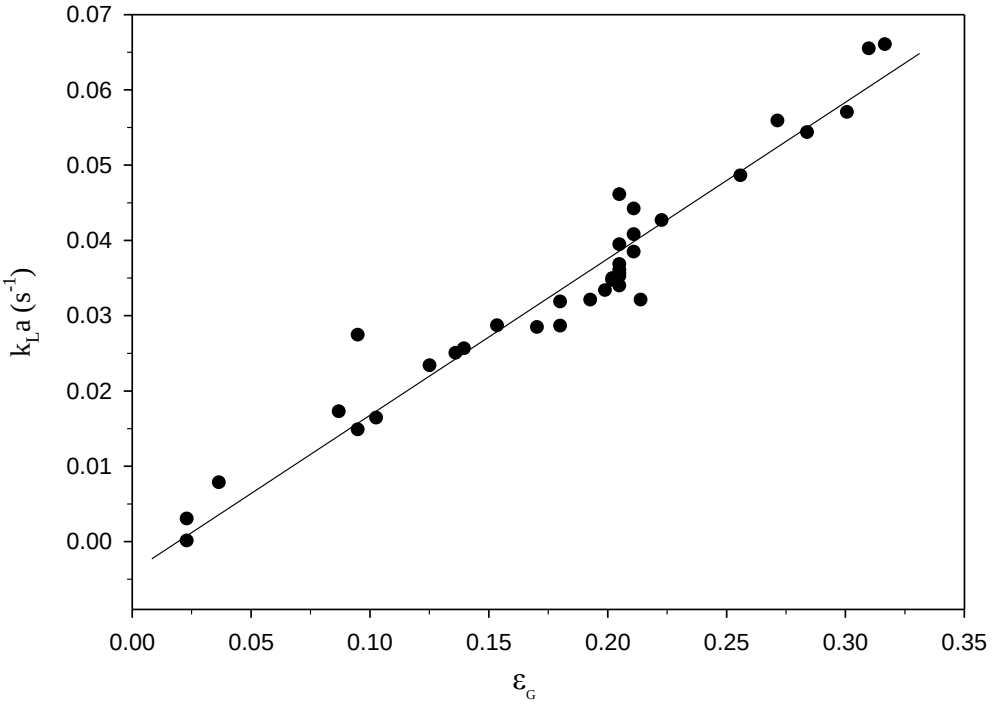

Figure 9 Plot of ozone-water mass transfer coefficients as a function of gas hold-up obtained using the three reactor arrangements, under various input gas flow rates and oscillation conditions.

3.2 Ozone-water mass transfer under continuous flow conditions

These experiments were performed under continuous flow conditions to evaluate the effect of superficial water velocity on k_La and mass transfer efficiency *(MTE).*

3.2.1 The effect of the input gas and water flow rates on k_La

The baffled reactor was operated as a co-current up flow contactor to assess its performance with respect to ozone-water mass transfer. The ozone-water mass transfer coefficient was investigated at gas and liquid flow rates of 0.1 to 1.0 $dm^3\ min^{-1}$, and the results are shown in fig. 10. k_La was found to increase significantly with the input gas and water flow rates, and the highest k_La of 0.134 s^{-1} was observed at the highest flow rates. Interestingly, this value is 2 times greater than that achieved with the same reactor operated at the same input gas flow rate and without water throughput as was shown in fig. 5. This may be attributed to the

additional turbulence induced by water flow and to the potential acceleration of liquid film renewal at the interface, based on thin film renewal theory [24].

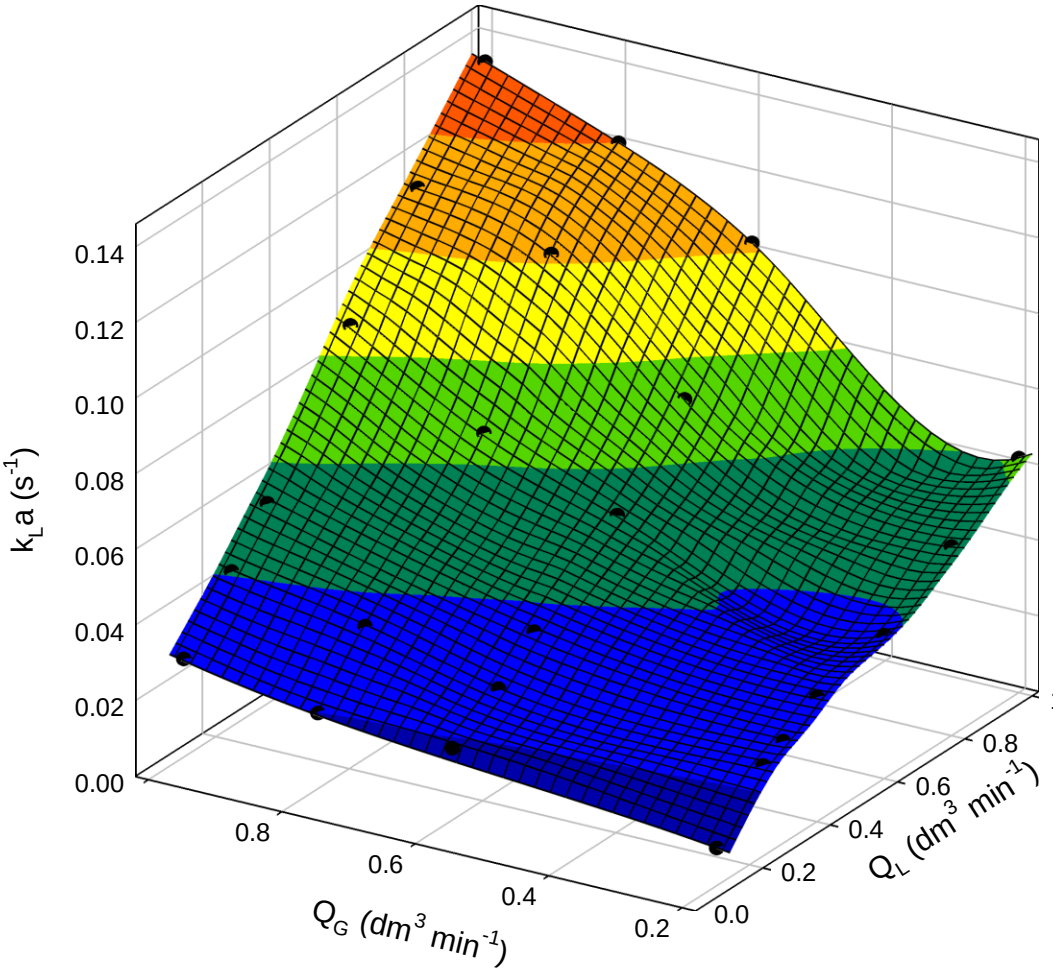

Figure 10 The variation in the ozone-water mass transfer coefficient of the baffled reactor as a function of the input gas and water flow rates.

In order to assess the oscillation effect on k_La under continuous flow conditions, the reactor was operated as a baffled reactor and as an OBR at a fixed input gas flow rate whilst varying the water flow rate, and the results are presented in fig. 11. As can be seen, oscillation enhanced k_La, and the enhancement was found to be almost constant at ca. 38-43% irrespective of water flow rate.

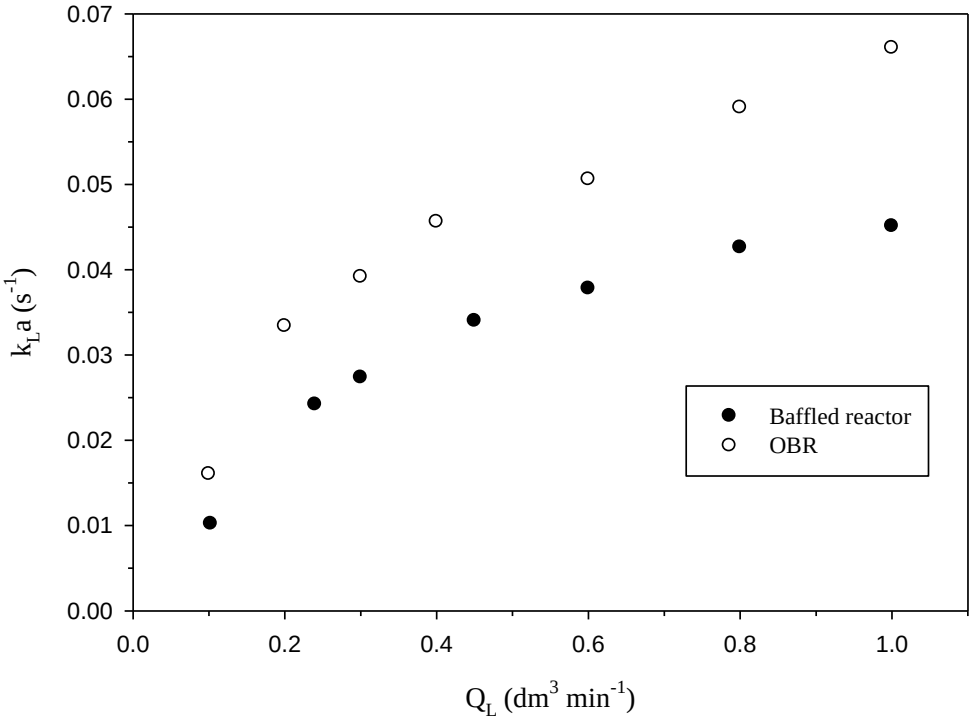

Figure 11 Plot of ozone-water mass transfer coefficient obtained using the baffled reactor without oscillation and the OBR as a function of input water flow rate. At Q_G = 0.2 dm^3 min^{-1} and $[O_3]_G$ = 29.8 mg dm^{-3}. The Re_o was fixed at 4600 in the case of the OBR.

3.2.2 The effect of the input gas and liquid flow rates on mass transfer efficiency (MTE)

The mass transfer efficiency (*MTE*), is the ratio of the mass of dissolved ozone to that dissipated via gas bubbling, and was determined according to:

$$\text{MTE } \% = ((Q_L \times [O_3]_L)/ (Q_G \times [O_3]_G)) \times 100 \quad (9)$$

Where Q_L and Q_G are the input water and gas flow rates (dm^3 min^{-1}), and $[O_3]_L$ and $[O_3]_G$ are the ozone concentrations in liquid and gaseous phases (mg dm^{-3}), respectively.

The effect of the input gas and water flow rates upon *MTE* was determined using the baffled reactor. The data is shown in fig. 12. From the figure, it can be seen that the mass transfer efficiency was found to increase proportionally with water flow rate and inversely to the gas flow rate. The highest mass transfer efficiency of 57% was obtained at the lowest input gas

flow rate, 0.1 dm^3 min^{-1}, and highest input water flow rate, 1.0 dm^3 min^{-1}. Operation of the baffled reactor at low input gas flow rate is desirable because of the high efficiency, lower cost of gas pumping and the reduction in power dissipation for ozone generation.

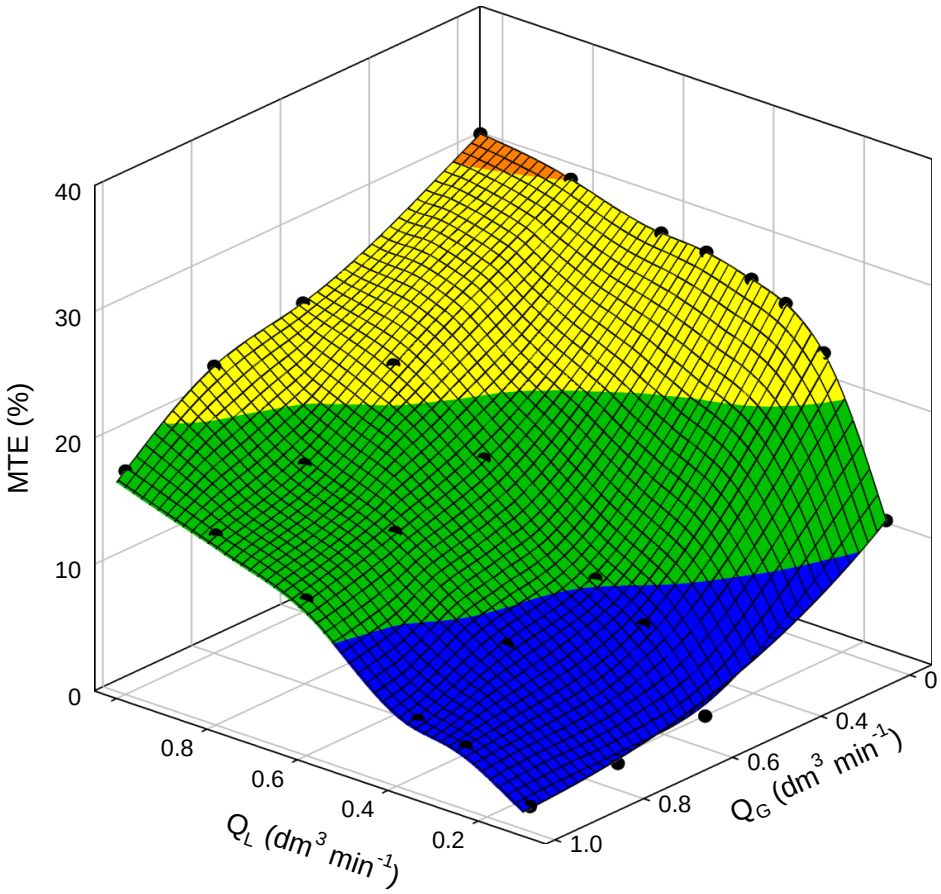

Figure 12 Ozone-water mass transfer efficiency as a function of the input gas and water flow rates obtained using the baffled reactor.

The effect of oscillation on *MTE* was extracted from fig.11 and the results so obtained are shown in fig.13. As can be seen from the figure, the effect of oscillation on *MTE* was found to be more important at water flow rates > 0.6 dm^3 min^{-1}. This may be attributed to the larger difference between the k_La values at high water flow rates as was seen in fig.12. The highest *MTE*, of a ca. 92%, was observed using the OBR at gas and water flow rates of 0.1 and 1.0 dm^3 min^{-1}. Table 4 shows the variation of *MTE* and steady state dissolved ozone concentrations at low input gas flow rate using the baffled reactor and OBR. The

enhancement so obtained at low superficial gas velocity may be attributed to the longer contacting time between the phases, and to the lower bubble collisions as discussed in section 3.1.4.

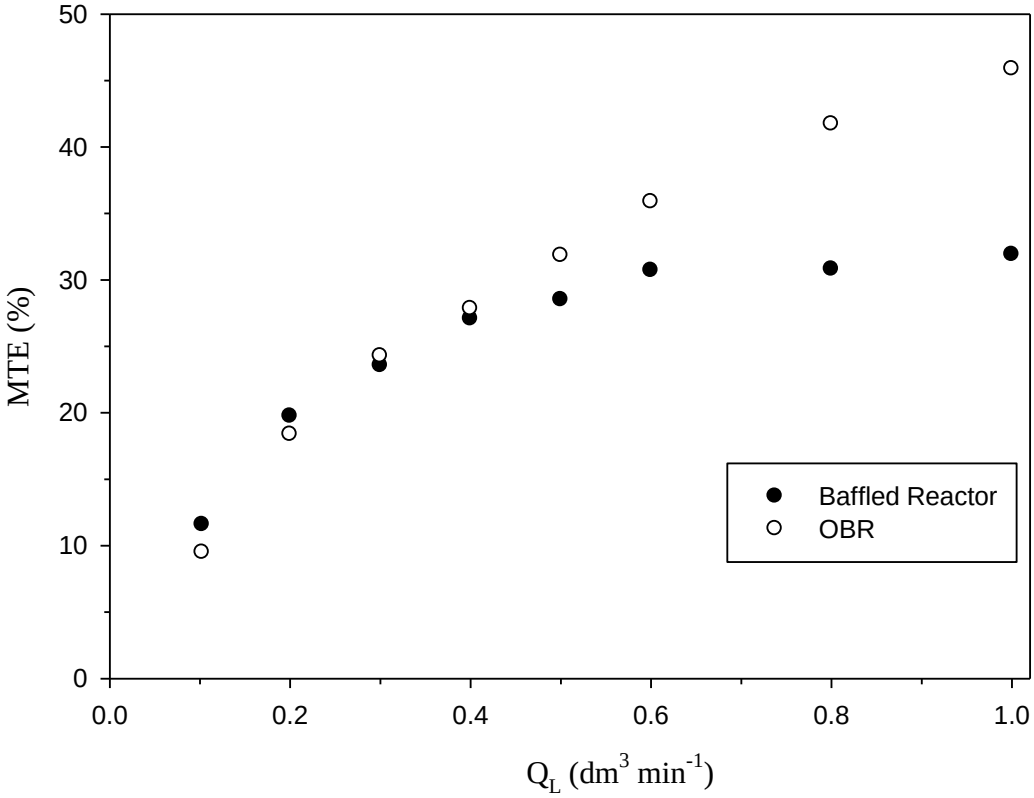

Figure 13 Plots of MTE obtained using the baffled reactor and the OBR as a function of input water flow rate; the conditions as for fig.11.

Table 4: The effect of the reactor arrangement and inputs gas and liquid flow rates on the dissolved ozone concentration and MTE. The Re_o was fixed at 4600 in the case of the OBR.

Reactor arrangement	*Q_G (dm^3 min^{-1})*	*Q_L (dm^3 min^{-1})*	*$[O_3]_G$ (mg dm^{-3})*	*$[O_3]_L$ (mg dm^{-3})*	*MTE (%)*
Baffled reactor	0.1	0.6	42.1	2.5	35.3
	0.1	1.0	31.5	1.8	57
OBR	0.1	0.6	42.1	4.8	67.8
	0.1	1.0	31.2	2.7	91.6

4. Conclusions

Ozone-water mass transfer was investigated under semi-batch conditions in a bubble column, a baffled column and an oscillatory baffled reactor. The OBR was demonstrated to be up to three and five times more efficient for ozone-water mass transfer than bubble and baffled column reactors respectively. The enhancement obtained with OBR over the baffled column reactor for ozone-water mass transfer was found to decline with gas flow rate due to changes in bubble flow pattern. Under continuous flow conditions, the performance of the baffled reactor and the OBR were found to increase with water and gas flow rates, probably due to increasing liquid turbulence and liquid film renewal. However, the mass transfer efficiency in both reactors was found to increase proportionally with water flow rate and inversely to the gas flow rates due to the decrease in contact time between the phases and to the acceleration of bubble collisions. The significant enhancements of k_La and *MTE* attained using the OBR under atmospheric pressure, using a short reactor length, and at low gas/liquid volumetric ratios make this type of reactor one of the most effective contactors for ozone-water mass transfer.

5. Acknowledgment

A. J. Al-Abduly wishes to thank Newcastle University and King Abdulaziz City for Science and technology (KACST) for technical and financial supports.

Notation

Re_o	oscillatory Reynolds number
St	Strouhal number
x_o	oscillation amplitude, mm
f	oscillation frequency, Hz
t	time, min
D_o	internal baffle diameter, mm
$[O_3]^*$	steady state dissolved ozone concentration, mg dm^{-3}
$[O_3]_L$	dissolved ozone concentration, mg dm^{-3}
$[O_3]_G$	gaseous phase ozone concentration, mg dm^{-3}
Q_L	liquid flow rate, dm^3 min^{-1}
Q_G	gas flow rate, dm^3 min^{-1}
k_La	volumetric mass transfer coefficient, s^{-1}
U_G	gas superficial velocity, cm s^{-1}
U_L	liquid superficial velocity, cm s^{-1}
h	steady state liquid height during the ozonation, cm
h_o	liquid height before ozonation, cm
$MTE\%$	mass transfer efficiency, %

Greek letters

ε_G	gas hold-up
p	liquid density, kg m^{-1}
μ	liquid viscosity, kg m^{-1} s^{-1}

References

[1] J. Hoigne, H. Bader, W.R. Haag, J. Staehelin, Rate Constants of Reactions of Ozone with Organic and Inorganic-Compounds in Water .3. Inorganic-Compounds and Radicals, Water Res, 19 (1985) 993-1004.

[2] K. Ikehata, M.G. El-Din, Degradation of recalcitrant surfactants in wasterwater by ozonation and advances oxidation processes: A review, Ozone-Sci Eng, 26 (2004) 327-343.

[3] T.E. Agustina, H.M. Ang, V.K. Vareek, A review of synergistic effect of photocatalysis and ozonation on wastewater treatment, J Photoch Photobio C, 6 (2005) 264-273.

[4] P. Paraskeva, N.J.D. Graham, Ozonation of municipal wastewater effluents, Water Environ Res, 74 (2002) 569-581.

[5] G. Tiwari, P. Bose, Determination of ozone mass transfer coefficient in a tall continuous flow counter-current bubble contactor, Chem Eng J, 132 (2007) 215-225.

[6] H.M. Letzel, J.C. Schouten, R. Krishna, C.M. van den Bleek, Gas holdup and mass transfer in bubble column reactors operated at elevated pressure, Chem Eng Sci, 54 (1999) 2237-2246.

[7] T. Mizuno, H. Tsuno, Evaluation of Solubility and the Gas-Liquid Equilibrium Coefficient of High Concentration Gaseous Ozone to Water, Ozone-Sci Eng, 32 (2010) 3-15.

[8] A.K. Bin, B. Duczmal, P. Machniewski, Hydrodynamics and ozone mass transfer in a tall bubble column, Chem Eng Sci, 56 (2001) 6233-6240.

[9] Y.Q. Qiu, C.H. Kuo, M.E. Zappi, Performance and simulation of ozone absorption and reactions in a stirred-tank reactor, Environ Sci Technol, 35 (2001) 209-215.

[10] V. Farines, S. Baig, J. Albet, J. Molinier, C. Legay, Ozone transfer from gas to water in a co-current upflow packed bed reactor containing silica gel, Chem Eng J, 91 (2003) 67-73.

[11] M.S.N. Oliveira, X. Ni, Gas hold-up and bubble diameters in a gassed oscillatory baffled column, Chem Eng Sci, 56 (2001) 6143-6148.

[12] M.R. Hewgill, M.R. Mackley, A.B. Pandit, S.S. Pannu, Enhancement of Gas-Liquid Mass-Transfer Using Oscillatory Flow in a Baffled Tube, Chem Eng Sci, 48 (1993) 799-809.

[13] X. Ni, S. Gao, R.H. Cumming, D.W. Pritchard, A Comparative-Study of Mass-Transfer in Yeast for a Batch Pulsed Baffled Bioreactor and a Stirred-Tank Fermenter, Chem Eng Sci, 50 (1995) 2127-2136.

[14] X. Ni, G. Brogan, A. Struthers, D.C. Bennett, S.F. Wilson, A systematic study of the effect of geometrical parameters on mixing time in oscillatory baffled columns, Chem Eng Res Des, 76 (1998) 635-642.

[15] A.P. Harvey, M.R. Mackley, P. Stonestreet, Operation and optimization of an oscillatory flow continuous reactor, Ind Eng Chem Res, 40 (2001) 5371-5377.

[16] X. Ni, P. Gough, On the discussion of the dimensionless groups governing oscillatory flow in a baffled tube, Chem Eng Sci, 52 (1997) 3209-3212.

[17] H.D. Zhou, D.W. Smith, Ozone mass transfer in water and wastewater treatment: Experimental observations using a 2D laser particle dynamics analyzer, Water Res, 34 (2000) 909-921.

[18] K. Rakness, G. Gordon, B. Langlais, W. Masschelein, N. Matsumoto, Y. Richard, C.M. Robson, I. Somiya, Guideline for measurement of ozone concentration in the process gas from an ozone generator, Ozone-Sci Eng, 18 (1996) 209-229.

[19] S. Stucki, H. Baumann, H.J. Christen, R. Kotz, Performance of a Pressurized Electrochemical Ozone Generator, J Appl Electrochem, 17 (1987) 773-778.

[20] W. Li, S.T. Oyama, Mechanism of ozone decomposition on a manganese oxide catalyst. 2. Steady-state and transient kinetic studies, J Am Chem Soc, 120 (1998) 9047-9052.

[21] M. Kuosa, A. Laari, J. Kallas, Determination of the Henry's coefficient and mass transfer for ozone in a bubble column at different pH values of water, Ozone-Sci Eng, 26 (2004) 277-286.

[22] M.S.N. Oliveira, X.W. Ni, Effect of hydrodynamics on mass transfer in a gas-liquid oscillatory baffled column, Chem Eng J, 99 (2004) 59-68.

[23] R. Krishna, J.M. van Baten, Mass transfer in bubble columns, Catal Today, 79 (2003) 67-75.

[24] P. V. Danckwerts, *Significance of Liquid-Film Coefficients in Gas Absorption,* Ind Eng Chem Res, 43 (1951) 1460-1467.

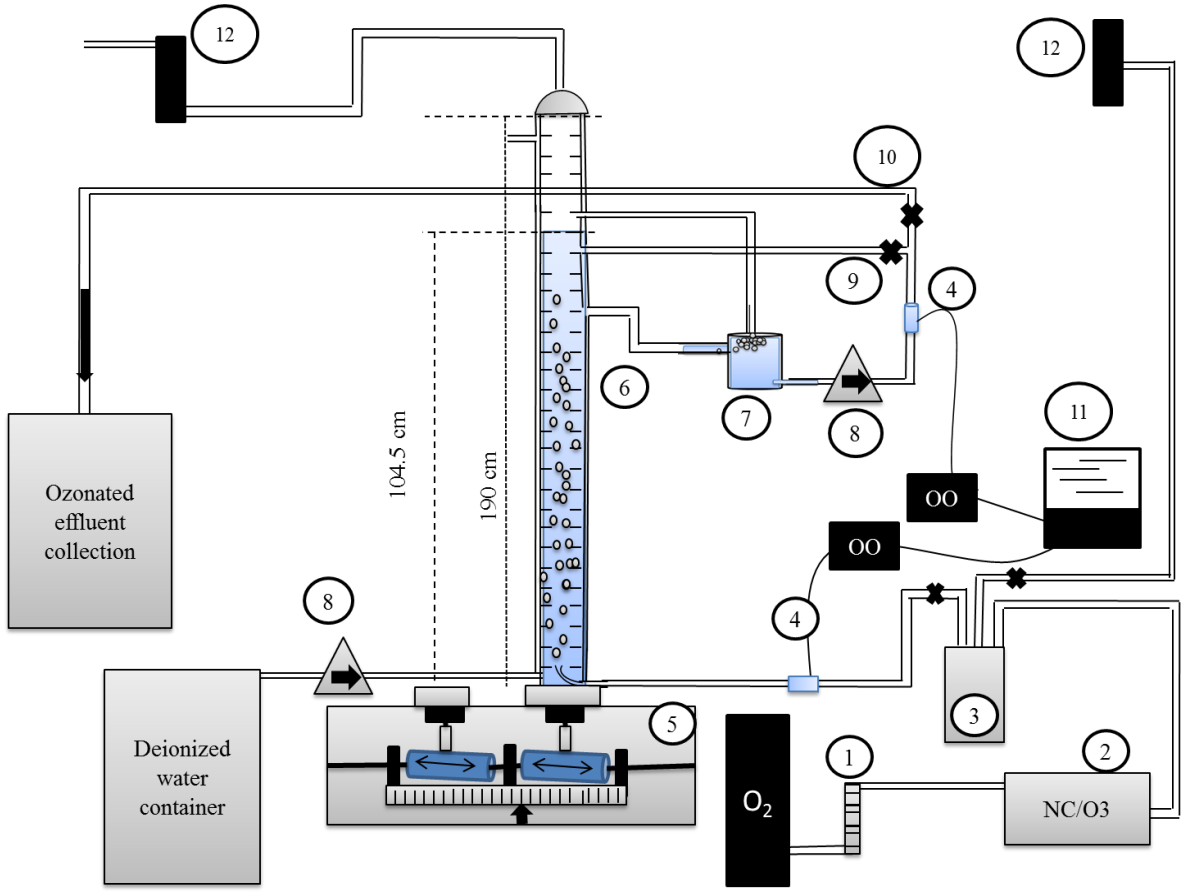

Figure 1 The system setup: (1) gas flow meter, (2) novel cell-ozone generator (PBDBD), (3) ozone distribution cell, (4) Ocean Optics flow cells, (5) oscillation supplying motor, (7) bubble removing cell, (8) peristaltic tubing pumps, (9) return port, (10) outlet port, (11) data collection station and (12) ozone destruction cells.

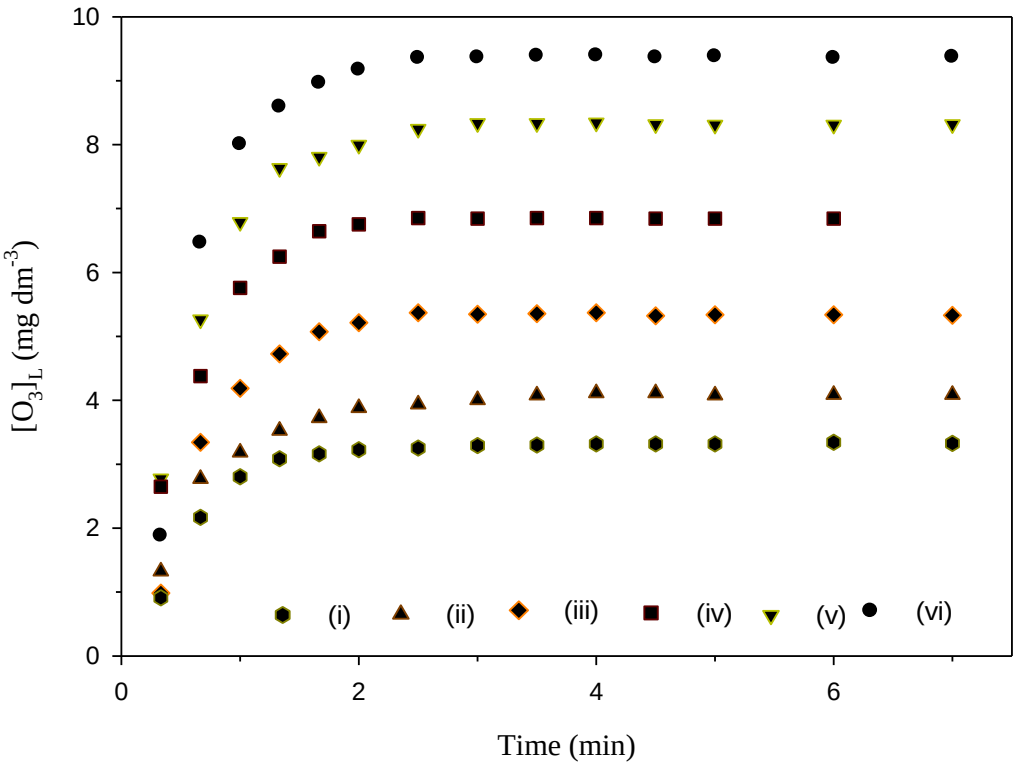

Figure 2 The change in dissolved ozone with time as a function of the input ozone concentration using the baffled reactor. Q_G was 1.0 dm^3 min^{-1} and $[O_3]_G$ were: (i) 11.3, (ii) 13.3, (iii) 18.1, (iv) 22.4, (v) 27.7 and (vi) 33.3 mg dm^{-3}.

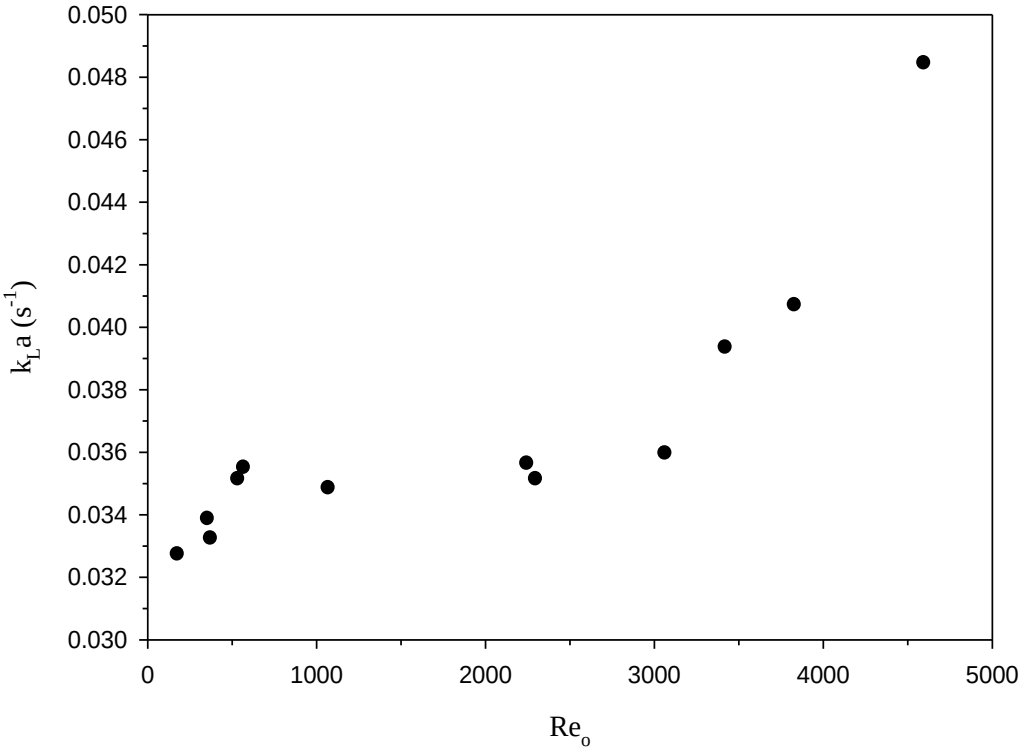

Figure 3 A plot of ozone-water mass transfer coefficient as a function of Re_o. The $[O_3]_G$ was 62.0 mg dm^{-3} and Q_G was 1.0 dm^3 min^{-1}.

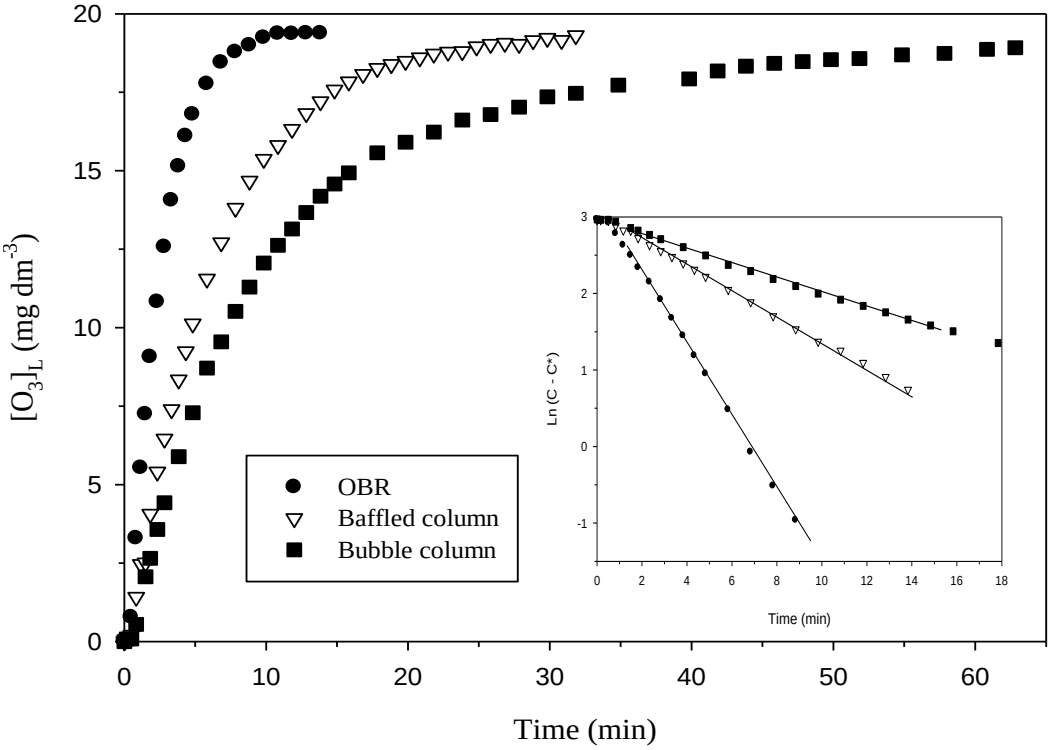

Figure 4 Ozone-water dissolution as a function of running time and reactor arrangement. $[O_3]_G$ was 65 mg dm^{-3} at Q_G = 0.1 dm^3 min^{-1}. Re_o was fixed at 4600 in the case of the OBR. The inset shows the plots of Ln ($[O_3]^*$-$[O_3]_L$) vs. time used for the determination of k_La (see text for details).

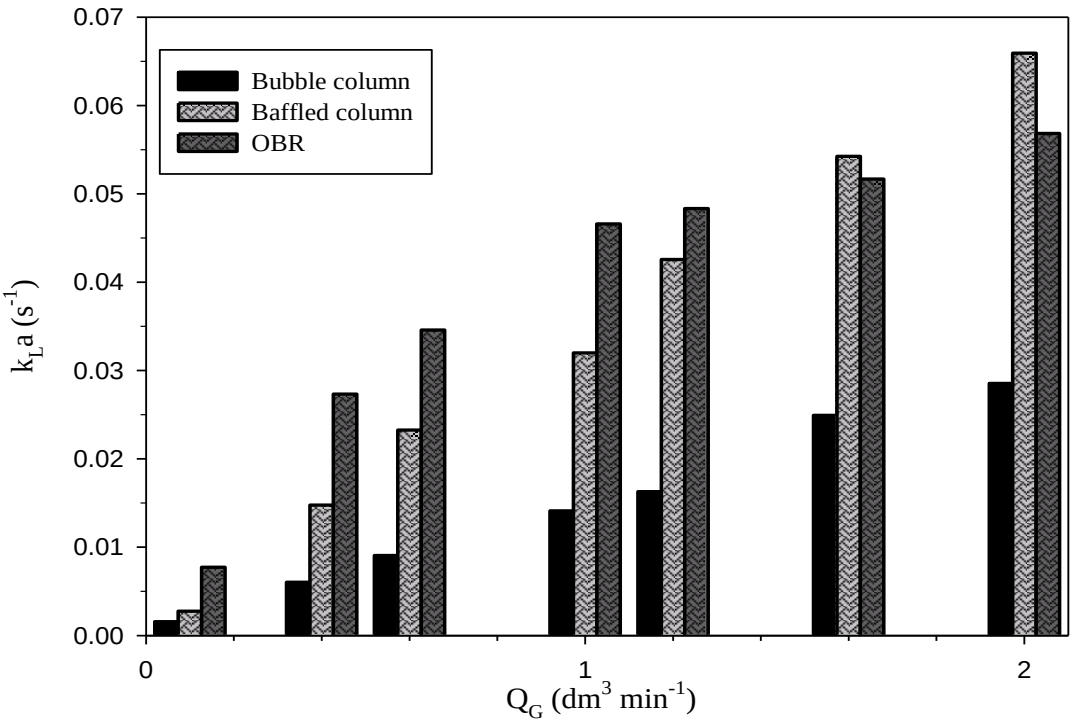

Figure 5 Ozone-water mass transfer coefficients as a function of the reactor arrangement and input gas flow rate. Re_o was fixed at 4600 in the case of the OBR.

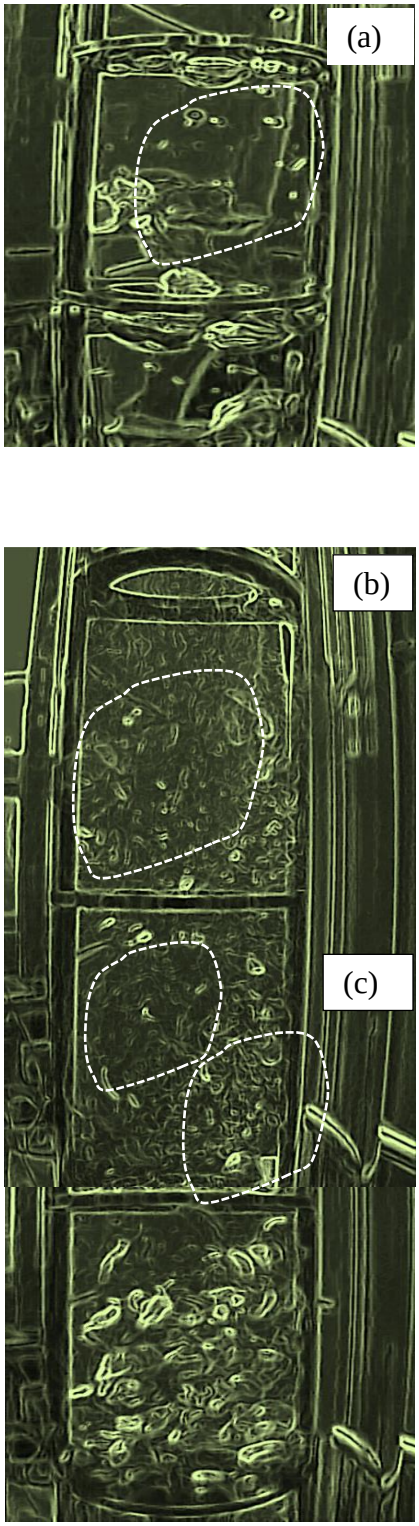

Figure 6 Gas flow patterns observed using the baffled reactor at 0.4 dm^3 min^{-1} (a) and the OBR at 0.4 dm^3 min^{-1}(b) and 1.6 dm^3 min^{-1} (c). The Re_o was fixed at 4600 in both (b) and (c).

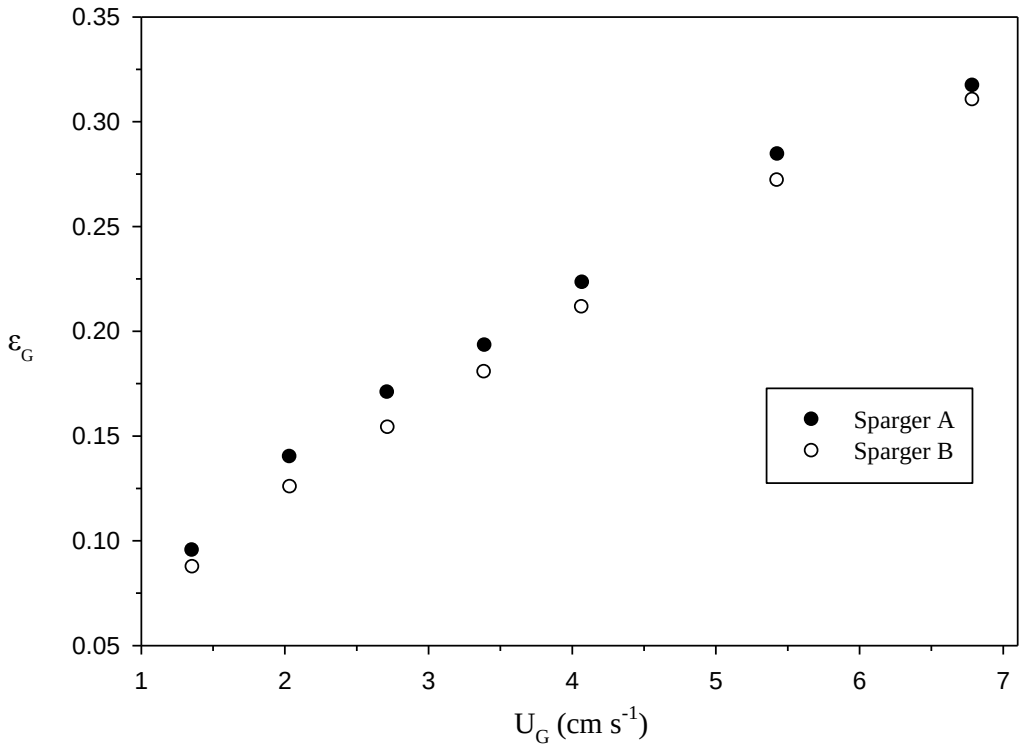

Figure 7 Plot of gas hold-up as a function of the gas superficial velocity obtained using spargers A and B in the baffled reactor.

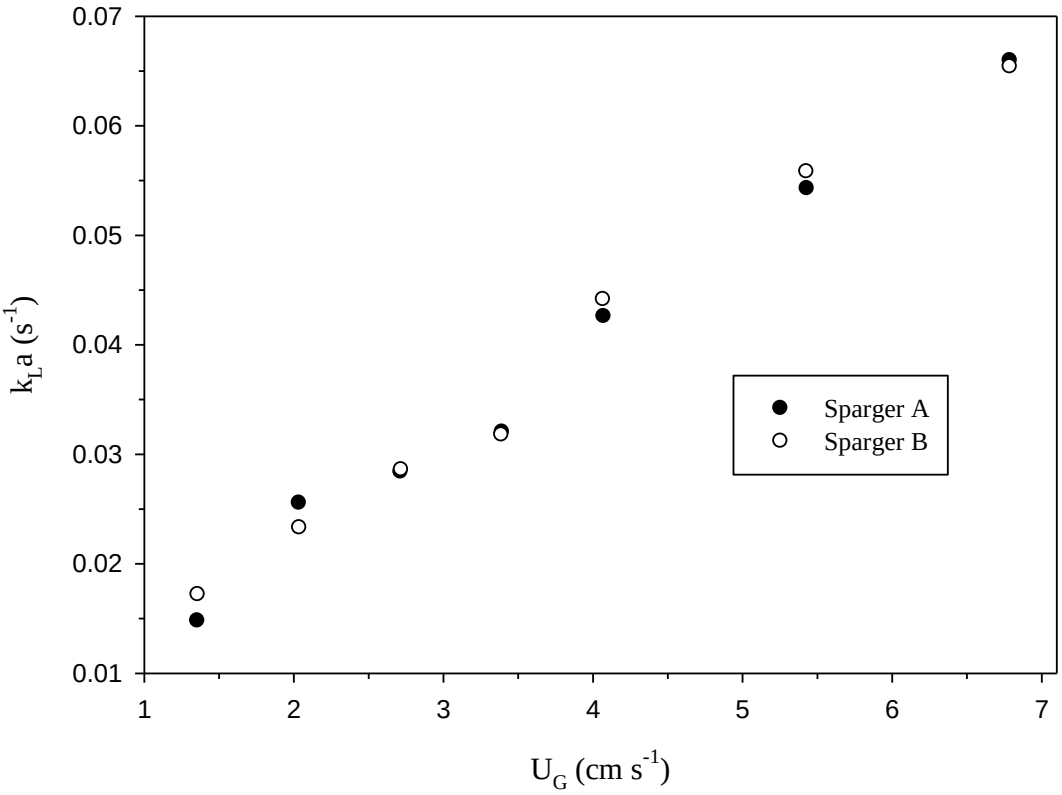

Figure 8 Plot of k_La as a function of gas superficial velocity and diffuser type using the baffled reactor.

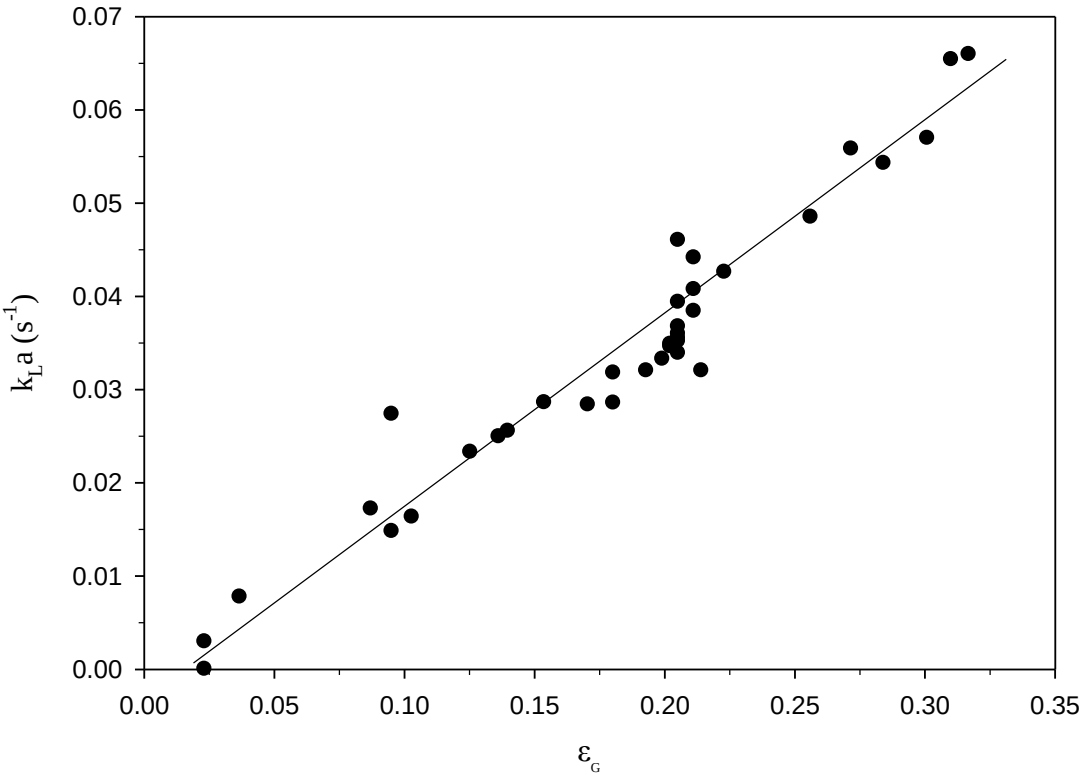

Figure 9 Plot of ozone-water mass transfer coefficients as a function of gas hold-up obtained using the three reactor arrangements, under various input gas flow rates and oscillation conditions.

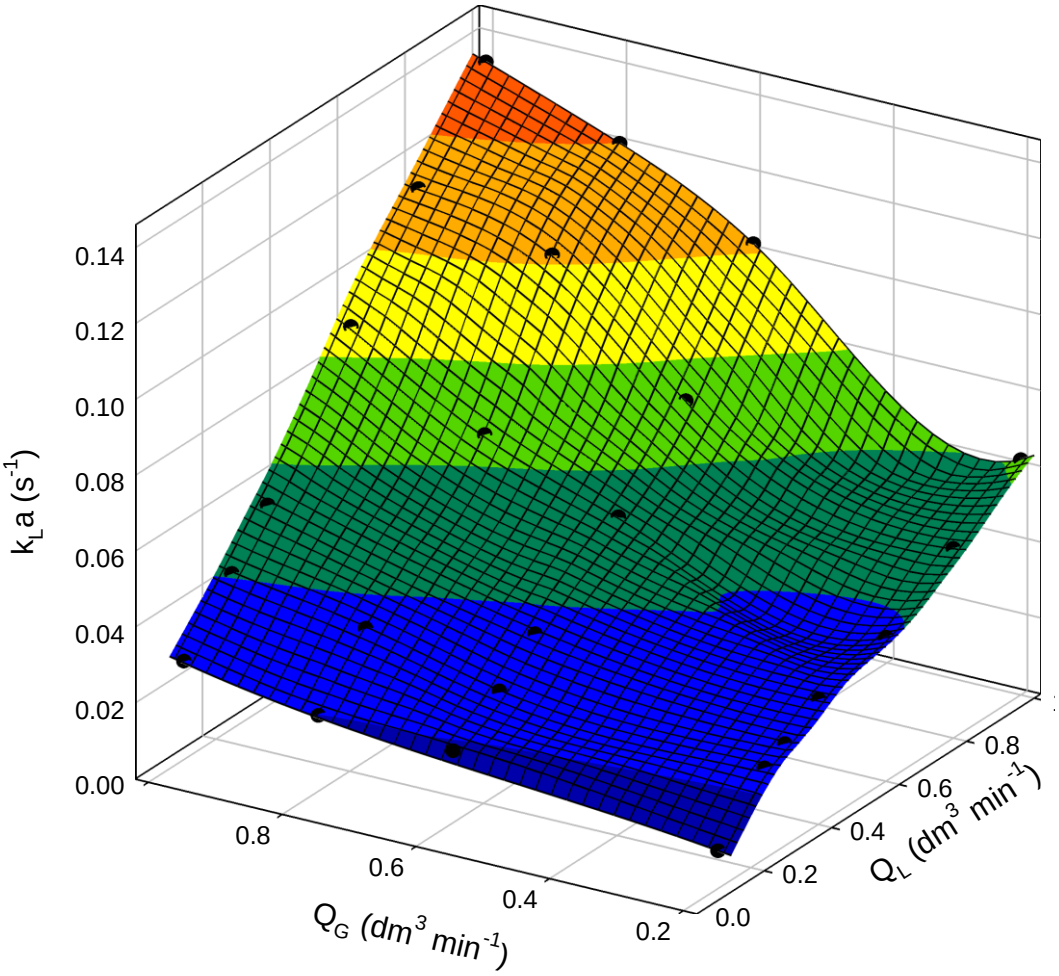

Figure 10 The variation in the ozone-water mass transfer coefficient of the baffled reactor as a function of input gas and water flow rates.

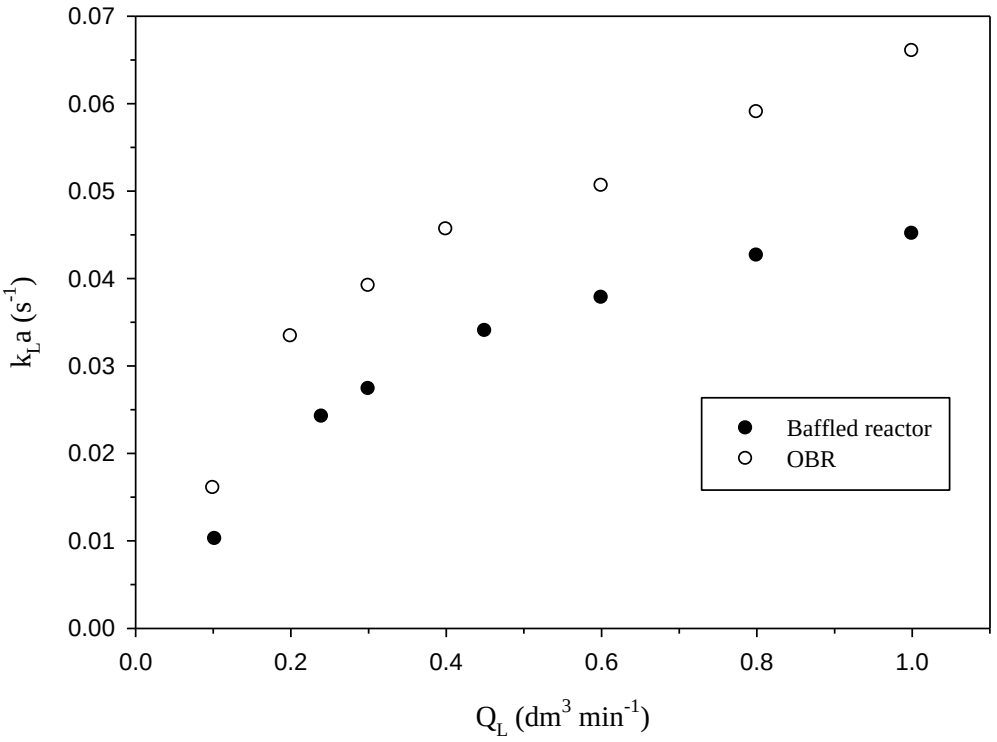

Figure 11 Plot of ozone-water mass transfer coefficient obtained using the baffled reactor without oscillation and the OBR as a function of input water flow rate. At Q_G = 0.2 dm^3 min^{-1} and $[O_3]_G$ = 29.8 mg dm^{-3}. The Re_o was fixed at 4600 in the case of the OBR.

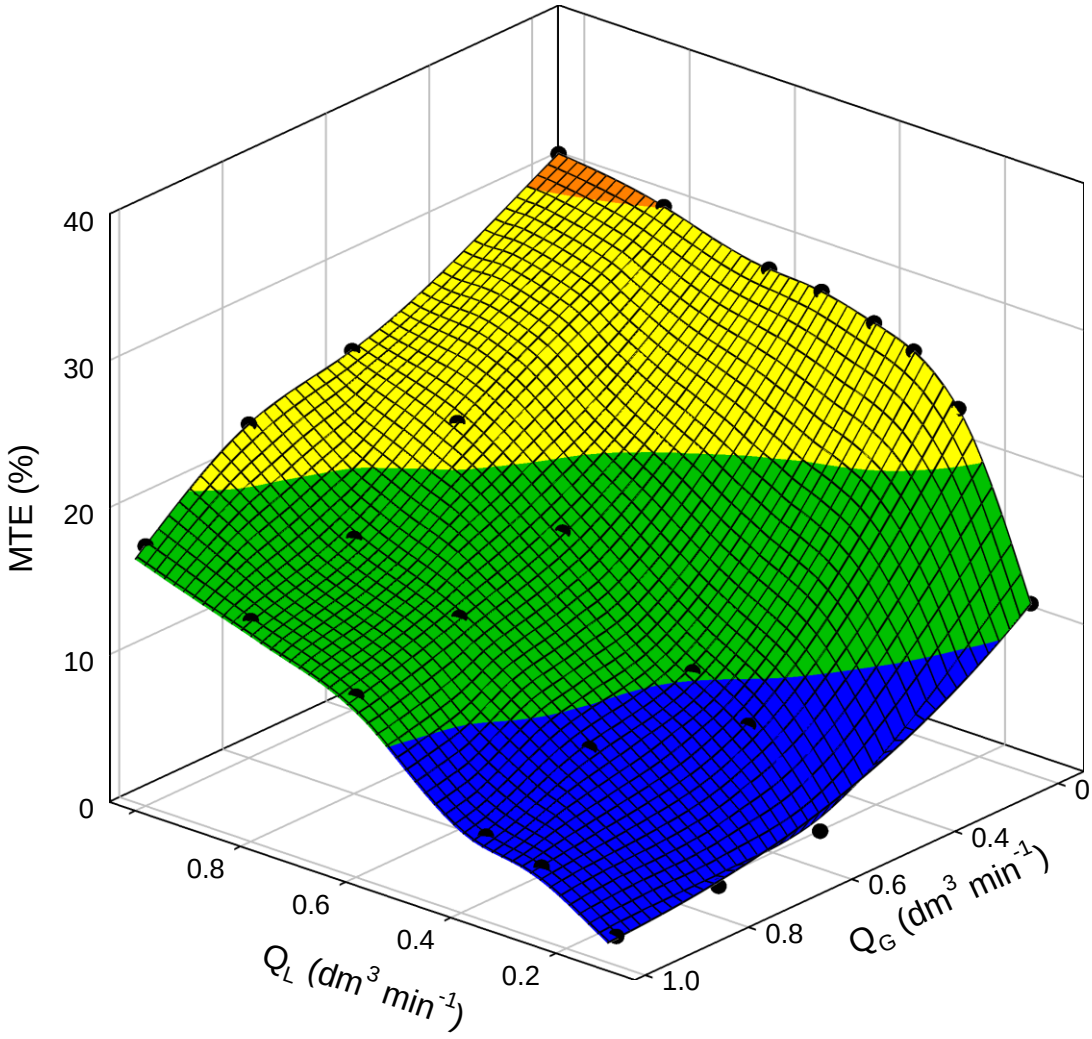

Figure 12 Ozone-water mass transfer efficiency as a function of input gas and water flow rates obtained using the baffled reactor.

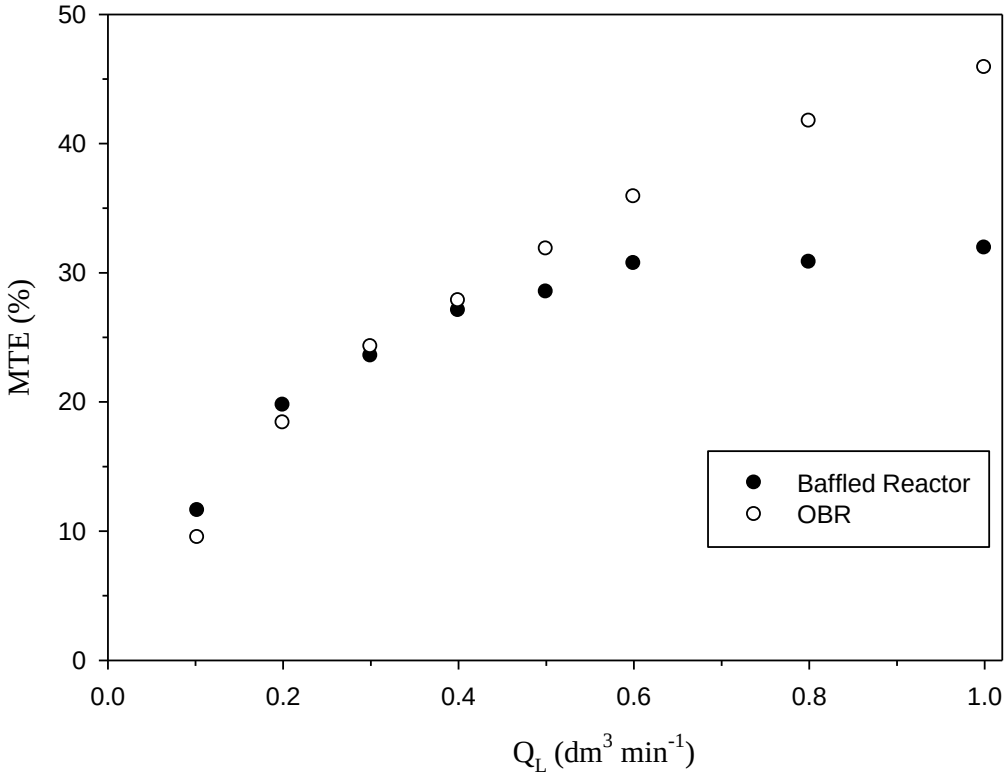

Figure 13 Plots of MTE obtained using the baffled reactor and the OBR as a function of input water flow rate; the conditions as for fig.11.

Table 1: Summary of the experimental conditions employed.

Parameter	*Semi-batch*	*Continuous*
Q_G ($dm^3\ min^{-1}$)	0.1 - 2.0	0.1 - 1.2
U_G ($cm\ s^{-1}$)	0.3 - 6.8	0.3 - 3.4
Q_L ($dm^3\ min^{-1}$)	0.0	0.1 - 1.0
U_L ($cm\ s^{-1}$)	0.0	0.3 – 3.4
$[O_3]_G$ ($mg\ dm^{-3}$)	11.3 - 64.5	11.3 - 64.5
Sampling rate ($dm^3\ min^{-1}$)	0.18	$= Q_L$

Table 2: The oscillation conditions employed in this work.

	Semi-batch	*Continuous*
Frequency (Hz)	1.2 - 5.0	5.0
Amplitude (mm)	1.0 - 6.0	6.0
Re_o	178 - 4600	4600
St	1.99 - 0.33	0.33

Table 3: k_La values at different input ozone concentrations, Q_G = 1.0 $dm^3\ min^{-1}$, using the baffled reactor.

$[O_3]_G$ ($mg\ dm^{-3}$)	$[O_3]^*$ ($mg\ dm^{-3}$)	k_La (min^{-1})	*Henry's constant* ($atm\ dm^3\ mol^{-1}$)
11.3	3.34	1.99	81.4
13.3	4.29	1.99	74.6
18.1	5.37	1.94	81.1
22.4	6.85	1.93	78.7
27.7	8.33	1.91	80.0
33.3	9.39	2.00	85.3

Table 4: The effect of the reactor arrangement and inputs gas and liquid flow rates on the dissolved ozone concentration and MTE. The Re_o was fixed at 4600 in the case of the OBR.

Reactor arrangement	Q_G *(dm^3 min^{-1})*	Q_L *(dm^3 min^{-1})*	$[O_3]_G$ *(mg dm^{-3})*	$[O_3]_L$ *(mg dm^{-3})*	*MTE (%)*
Baffled reactor	0.1	0.6	42.1	2.5	35.3
	0.1	1.0	31.5	1.8	57
OBR	0.1	0.6	42.1	4.8	67.8
	0.1	1.0	31.2	2.7	91.6